Title no. 109-S33

Linear Analysis of Concrete Frames Considering Joint Flexibility

by Anna C. Birely, Laura N. Lowes, and Dawn E. Lehman

Linear analysis is the first—and sometimes only—analysis method used to support the seismic design and evaluation of reinforced concrete (RC) buildings. Standards such as ASCE/SEI 41-06 provide recommendations for modeling structures as part of a linear analysis. These include appropriate effective stiffness values to be used for frame members to simulate the reduced stiffness due to cracking and frame-member rigid offset lengths to be used within the beam-column joint region to simulate the increased stiffness of this zone. While significant research has been conducted to develop and validate appropriate effective stiffness values for beams and columns, comparatively little research has addressed the simulation of beam-column joint rigidity or the validation of linear analysis methods for the prediction of frame response. The research presented herein used data from prior laboratory tests of RC frame subassemblages to evaluate existing recommendations and develop improved recommendations for simulating joint flexibility to improve the accuracy of linear response modeling.

Keywords: analytical models; beam-column joints; effective stiffness; rigid offsets.

INTRODUCTION

During an earthquake, a reinforced concrete (RC) moment frame is subject to moment reversal in the beams and columns at the joints. This results in high shear and bond stress demands in the joint, which in turn affects the overall performance of the moment frame. Experimental results[1-12] show that joint demands result in joint damage, reduced frame stiffness and, in some cases, premature strength loss. Thus, to accurately represent structural behavior, engineers must simulate the stiffness and strength of joints, beams, and columns in RC frame models.

This study considered the modeling of frame subassemblages for linear analysis, which is typically the first—and, in some cases, the only—analysis approach used in seismic design and evaluation. Typically, a model used for linear analysis of a frame comprises beam-column elements that simulate flexural, shear, and axial response. These elements are oriented along beam and column centerlines and connected at nodes at the center of the joint. Rigid offsets are introduced at the ends of the members within the joint volume to simulate the stiffness of the joint. Creation of the typical model requires two primary estimations by the engineer: 1) effective stiffness values for the beams and columns; and 2) the length of the rigid offset within the joint. Recommendations for both are provided in standards such as ASCE/SEI 41-06.[13] Research has been conducted to validate stiffness recommendations for beams and columns; however, research investigating appropriate rigid offset length recommendations and the combination of frame-member effective stiffnesses and rigid offset lengths to represent moment frame behavior is limited. This research was undertaken to develop appropriate recommendations for this important aspect of frame modeling. The models considered herein are limited to the pre-yield range of a structure.

The literature[14-22] contains a wide range of nonlinear models for simulating the earthquake response of RC beam-column joints as part of a frame analysis. Modeling the elastic stiffness of a joint depends on the nonlinear modeling approach used; an example of a different modeling approach and the corresponding elastic joint stiffness is presented by the authors elsewhere.[23] Common linear models use offsets at the end of frame members to create a rigid region within the joint. Few sources provide recommendations for the length of the offsets. ASCE/SEI 41-06[13] recommends a rigid offset length of: 1) the full dimension of the joint in the beams; 2) the full joint dimension of the joint in the columns; or 3) half the dimension in both the beams and columns. A distinction between these is made on the basis of the relative moment strengths of the beams and columns. Prior to publication of ASCE/SEI 41-06,[13] similar recommendations were available to engineers in the report, "Pre-Standard and Commentary for the Seismic Rehabilitation of Buildings (FEMA 356),"[24] with full joint dimensions used as the offset lengths for all joints. Neither of these recommendations has been verified using an extensive experimental data set.

This study investigated the performance of linear frame modeling using an extensive set of frame subassemblage tests, performed by others, that included a wide range of joint parameters. First, the subassemblages were modeled using centerline models (no offsets) and using offsets to define the entire joint region as rigid. These models provided upper and lower bounds on the performance of frame-member effective stiffness values in predicting the response of the moment frame subassemblages. Next, the rigid offset recommendations provided by FEMA 356[24] and ASCE/SEI 41-06[13] were evaluated. The results confirmed that the ASCE/SEI 41-06[13] results provided the more accurate prediction, as expected. Finally, new offset length recommendations were developed to further improve the prediction of subassemblage behavior. In developing these recommendations, the offset length was considered to be a function of joint design parameters. Different recommendations are made for joints that are designed in accordance with ACI 318-08[25] and those that are not. Specimens that exhibited brittle behavior in the laboratory were found to require shorter offset lengths than those that exhibited ductile behavior. To simulate this response in the model, criteria

Anna C. Birely *is a PhD Candidate in the Department of Civil and Environmental Engineering at the University of Washington, Seattle, WA. She received her BS from the University of Colorado, Boulder, Boulder, CO, and her MS from the University of Washington. Her research interests include modeling of existing concrete structures.*

ACI member **Laura N. Lowes** *is an Associate Professor in the Department of Civil and Environmental Engineering at the University of Washington. She received her BS from the University of Washington and her MS and PhD from the University of California, Berkeley, Berkeley, CA. She is a member of ACI Committee 369, Seismic Repair and Rehabilitation, and Joint ACI-ASCE Committees 445, Shear and Torsion; and 447, Finite Element Analysis of Reinforced Concrete Structures. Her research interests include numerical modeling of concrete structures and earthquake engineering.*

ACI member **Dawn E. Lehman** *is an Associate Professor in the Department of Civil and Environmental Engineering at the University of Washington. She received her BS from Tufts University, Boston, MA, and her MEng and PhD from the University of California, Berkeley. She is a member of ACI Committees 341, Earthquake-Resistant Concrete Bridges; 374, Performance-Based Seismic Design of Concrete Buildings; and Joint ACI-ASCE Committee 352, Joints and Connections in Monolithic Concrete Structures. Her research interests include seismic design of reinforced concrete and composite construction.*

were developed that predict if the subassemblage will be ductile or brittle with 95% accuracy.

RESEARCH SIGNIFICANCE

Linear analysis of RC moment frames requires the specification of frame-member effective stiffnesses and rigid offset lengths within the joint. Standards[13,24] provide recommendations for these model parameters; however, the accuracy of these recommendations has not been evaluated using an extensive data set. In this study, data from laboratory tests of frame subassemblages were used to evaluate existing recommendations and develop new recommendations for the simulation of joint flexibility. The activities employed an assembled data set and subsets of specimens considered to exhibit a ductile, beam-controlled response and brittle, joint-controlled response. Criteria for predicting brittle or ductile response modes are presented.
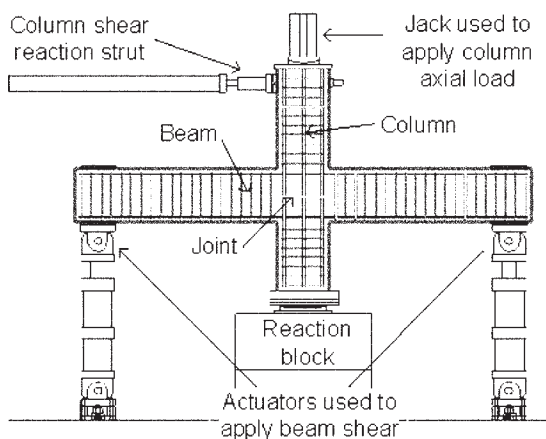

Fig. 1—Typical experimental test setup of beam-column joint subassemblage.

EXPERIMENTAL DATA SET

Accurate evaluation of existing models and validation of proposed models for frame analysis requires an extensive experimental data set that includes laboratory tests of frame subassemblages with a wide range of design parameters. In this study, a subset of the frame subassemblage data set assembled by Mitra and Lowes[21] was used. The data set used for this study included 45 interior beam-column joint subassemblages tested by 11 research teams.[1-12] Figure 1 shows a typical test specimen in the laboratory, consisting of two beams and two columns that extend from the joint to the point of inflection (half of the full length of the member). Subassemblages were subjected to reversed cyclic loading intended to represent earthquake loading, with loads applied either at the end of the beams or the top of the column. Most subassemblages were also subjected to simulated gravity load, which was applied through the column. The subassemblages included in the data set did not include lightweight concrete, slabs, smooth reinforcing steel, or transverse beams. Specimen response was controlled by beam yielding and/or joint damage; specimens exhibiting beam shear, column flexure, or column splice damage modes were not included in the data set.

Table 1 provides summary statistics of the design and response data for the test specimens included in the data set. Details of the data set are provided in Table A1 in the Appendix.[*]

Engineering characteristics of test specimen

The results of previous research and current design codes suggest that a number of factors may determine joint performance. As part of this study, the following characteristics and design parameters were considered:

1. *Scale factor*—To assess the impact of the specimens' scale on observed response, a scale factor was computed using the column longitudinal bar size and the assumption that a No. 8 (1.0 in. [25 mm] diameter) bar represented full scale.

2. *Normalized design shear stress τ*—ACI 352R-02[26] recommends that joint shear stress demand be computed as follows in design

$$\tau = \frac{1}{\sqrt{f_c'}h_c b_j}\alpha\left(f_y\left(A_s^{top} + A_s^{bot}\right) - V_n\right)\sqrt{\text{psi}}\left(\sqrt{\text{MPa}}\right) \quad (1)$$

where f_c' is the nominal concrete compressive strength; h_c is the height of the column; b_j is the out-of-plane dimension of the joint; f_y is the nominal yield strength of the beam longitudinal steel; A_s^{top} and A_s^{bot} are the longitudinal steel areas in the top and bottom of the beam, respectively; V_n

---

Table 1—Experimental data summary

	Scale	τ, √psi (√MPa)	$(h_c/d_b)_{norm}$	λ, √psi (√MPa)	ϕ_j	ρ_j	$\Sigma M_{nc}/\Sigma M_{nb}$	p
Minimum	0.50	5.50 (0.50)	7.20	12.60 (1.05)	0.00	0.00	0.70	0.02
Maximum	1.38	43.40 (3.60)	44.20	58.60 (4.87)	2.20	0.04	2.10	0.48
Mean	0.74	17.71 (1.54)	22.67	27.99 (2.32)	0.49	0.01	1.45	0.12
Coefficient of variation	0.38	0.49 (0.46)	0.42	0.47 (0.40)	1.06	0.97	0.23	0.83

is the column shear corresponding to the development of the nominal flexural strength of the beams framing into the joint; and α accounts for the actual-versus-nominal yield strength of the reinforcing steel and the hardening of the steel under loading. For this study, Eq. (1) was employed with *measured* concrete and steel strengths and $\alpha = 1.25/1.1$, where the 1.1 factor is used to approximate the design strengths from the measured properties, and the 1.25 factor is used to approximate the effect of strain hardening.

3. *Normalized beam longitudinal reinforcement anchorage ratio* $(h_c/d_b)_{norm}$—The normalized beam longitudinal reinforcement anchorage ratio is defined as

$$\left(\frac{h_c}{d_b}\right)_{norm} = \frac{66}{f_y}\frac{h_c}{d_b} \tag{2}$$

where d_b is the maximum diameter of beam longitudinal reinforcement; and all other variables are as defined previously. Because the measured—not design—yield strength is used, h_c/d_b is adjusted to allow for comparison with the ACI Code limit of 20. The adjustment factor is the expected yield strength (60 ksi [413 MPa] multiplied by the 1.1 factor recommended by ACI 352R-02[26]) divided by the measured yield strength of the steel.

4. *Bond ratio* λ—The bond ratio is defined as the normalized average beam-bar bond stress in the joint assuming the bar yields in compression and tension on either side of the joint

$$\lambda = \alpha\frac{f_y d_b}{2h_c\sqrt{f_c'}}\ \sqrt{psi}\ \left(\sqrt{MPa}\right) \tag{3}$$

where all variables are as defined previously; measured material properties are used; and the factor α is taken equal to 1.25/1.1 to account for the use of measured material properties.

5. *Normalized joint transverse reinforcement ratio* ϕ_j—The normalized joint transverse reinforcement ratio is the ratio of the yield force of the transverse reinforcement to the maximum joint shear force

$$\phi_j = \frac{A_{st}f_{yt}}{\tau_{max}h_c b_j} \tag{4}$$

where A_{st} is the total area of joint transverse reinforcement passing through a plane normal to the axis of beams; and f_{yt} is the measured strength of the joint transverse steel. The maximum joint shear stress τ_{max} is defined as

$$\tau_{max} = \frac{1}{h_c b_j}\left(\frac{M_L + M_R}{jh_b} - V_c^{max}\right) \tag{5}$$

where V_c^{max} is the maximum column shear applied in the laboratory; and M_L and M_R are, respectively, the corresponding moments in the left and right beams at the face of the joint.

6. *Joint reinforcement ratio* ρ_j—The joint reinforcement ratio is defined as

$$\rho_j = \frac{A_t}{s_t b_j} \tag{6}$$

where A_t is the area of one layer of joint transverse reinforcement passing through a plane normal to the axis of beams; s_t is the vertical spacing of hoops in the joint region; and b_j is the out-of-plane dimension of the joint.

7. *Moment ratio*—The moment ratio is the ratio of the sum of the flexural strengths of the columns to the beams framing into the joint

$$\alpha_M = \frac{\Sigma M_{nc}}{\Sigma M_{nb}} \tag{7}$$

where ΣM_{nc} and ΣM_{nb} are the sums of the nominal flexural strengths of the columns and beams, respectively, framing into the joint; and M_n is computed per ACI 318-08.[25]

8. *Column axial load ratio* p—The column axial load ratio is defined as

$$p = \frac{P}{A_g f_c'} \tag{8}$$

where P is the applied column axial load; and A_g is the gross area of the column.

Initial yield force and displacement data

The frame-member effective stiffness values and joint model recommendations were evaluated on the basis of the accuracy with which the experimental initial yield displacement of the frame subassemblage was simulated under application of the initial yield force. The initial yield force V_{yield} for each subassembledge was reported by Mitra and Lowes.[21] The yield force is defined as the column shear corresponding to the initial yield moment strength in the beams. The initial yield moments at the face of the joint were determined from a moment-curvature analysis of the beam cross sections using the reported material properties. The initial yield displacement Δ_{yield} was defined as the displacement corresponding to the initial yield force V_{yield} and was determined from the column shear load versus story drift history reported by the researchers. For some specimens in the data set, loading was applied to the beam and the equivalent column shear load versus story drift history was calculated from the reported beam response data. For specimens that did not reach theoretical yield, the maximum load and corresponding displacement were used instead. Figure 2 shows an example using the response history for PEER 0995,[4] in which the appropriate column shear and drift at initial yield of the beams are indicated by two lines. Table A2 in the Appendix lists the yield force and displacement values for each specimen in the data set.

ACI Code compliance

ACI 318-08[25] provides specifications for the design of joints in ordinary, intermediate, and special moment frames (SMFs). For this study, compliance with the SMF requirements, intended to maintain strength and integrity through severe earthquake loading, was considered. ACI-compliant joints meet the following requirements:
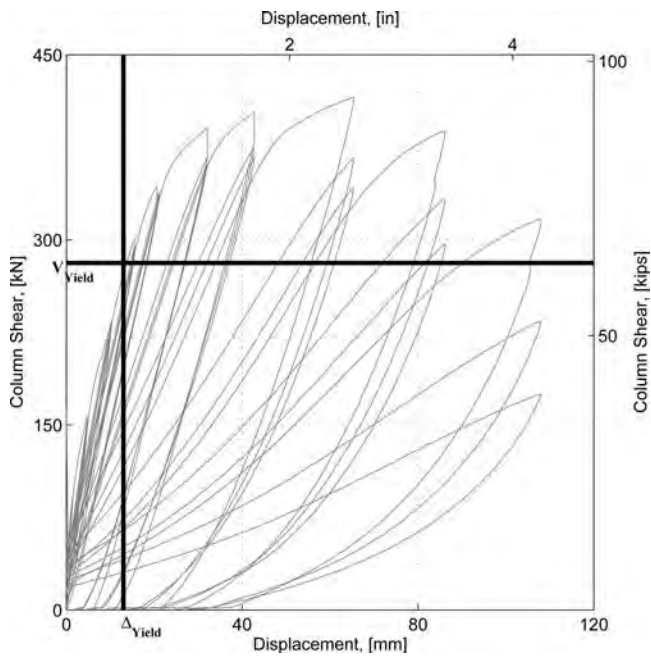
Fig. 2—PEER 0995 force-displacement history with theoretical initial yield point.
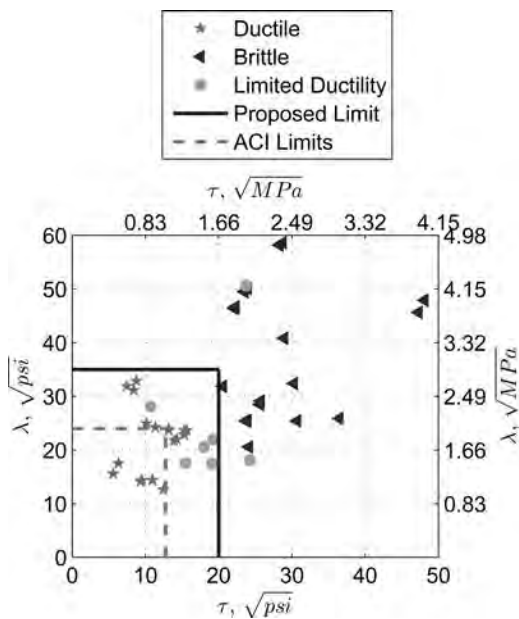

Fig. 3—Relationship of ductility classification to design shear stress and bond demand.

- A normalized beam longitudinal reinforcement anchorage ratio (($h_c/d_b)_{norm}$) of less than 20.
- A total cross-sectional area of the transverse reinforcement satisfying ACI 318-08, Section 21.6.4.4.
- Spacing of transverse reinforcement less than one-fourth the minimum joint dimension and less than six times the diameter of the longitudinal reinforcement, per ACI 318-08, Section 21.6.4.3; spacing requirements affected by specimen scale were not considered, as the true design scale was unknown for many specimens.
- Nominal joint shear demand V_u not greater than $\phi 15\sqrt{f_c'}A_j$, lb ($\phi 1.25\sqrt{f_c'}A_j$, N), where $\phi = 0.85$, f_c' is the

concrete compressive strength in psi, and A_j is the nominal area of the joint; V_u is computed as $V_u = \tau A_j\sqrt{f_c'}$ with τ computed per Eq. (1) and f_c' and A_j as defined previously.

Material strength limits were not considered in evaluating Code compliance. Joints not meeting the previous requirements were classified as ACI-noncompliant. Table A2 in the Appendix lists the ACI compliance status for each specimen.

Ductility classification

To support the model calibration, specimens were classified as brittle, ductile, or limited ductility:

- *Brittle*—Specimens for which maximum strength was less than the strength required to develop the maximum of the positive or negative beam yield moment, where the yield moment is defined by initial yielding of beam longitudinal reinforcement in tension.
- *Ductile*—Specimens not classified as brittle and with displacement ductility μ_Δ greater than 4.
- *Limited ductility*—Specimens not classified as brittle or ductile.

Displacement ductility μ_Δ was defined as

$$\mu_\Delta = \frac{\Delta_{90\%}}{\Delta_y} \qquad (9)$$

where $\Delta_{90\%}$ is the displacement at which 10% strength loss occurred as determined from the load-displacement history; and Δ_y is as defined previously. Using this classification procedure, 18 specimens were classified as brittle, 20 as ductile, and seven as limited ductility. The ductility classification of each specimen is provided in Table A2 in the Appendix.

Because brittle and ductile specimens were expected to require different modeling approaches, a method for predicting ductility classification, given frame and joint design parameters, was necessary. The design parameters and specimen characteristics listed in Table 1 were considered to determine such a method. It was concluded that ductility could be predicted from joint bond demand λ and design shear stress τ. Figure 3 shows bond stress demand λ plotted versus design shear stress τ for the specimens in the data set, with markers indicating the ductility classification. The solid lines in Fig. 3 indicate the proposed division between ductile and brittle specimens. A frame subassemblage with

$$\tau \leq 20\sqrt{psi}\ (1.66\sqrt{MPa}) \qquad (10)$$

$$\lambda \leq 35\sqrt{psi}\ (2.91\sqrt{MPa}) \qquad (11)$$

was predicted to exhibit ductile response or limited ductility. A frame subassemblage not meeting the criteria in Eq. (10) and (11) was predicted to exhibit brittle response. Using these criteria, the ductility classification was correctly identified for 95% of the subassemblages.

The limits defined by Eq. (10) and (11) are similar to the ACI 318-08[25] limits on joint shear demand and beam-bar anchorage length for the design of joints in SMFs described previously. The ACI Code requirement of joint shear

Table 2—Beam and column effective stiffness values

Name used in this study	Source	Flexural stiffness
FEMA 356	FEMA 356[24]	$0.5E_cI_g$ ($p \leq 30\%$) $0.7E_cI_g$ ($p \geq 50\%$)
ASCE 41	ASCE/SEI 41-06[13]	$0.3E_cI_g$ ($p \leq 10\%$) $0.7E_cI_g$ ($p \geq 50\%$)
Lower-bound	Elwood and Eberhard[30]	$0.2E_cI_g$ ($p \leq 10\%$) $0.7E_cI_g$ ($p \geq 50\%$)
Approximation A	Elwood and Eberhard[31]	$\alpha_{approx}^A E_c I_g$ $\alpha_{approx}^A = 0.2 + 1.3\left(\dfrac{P/A_gE_c}{\varepsilon_o}\right) + \rho n \leq 1.0$
Approximation B		$\alpha_{approx}^B E_c I_g$ $\alpha_{approx}^B = 0.35 + 1.3\left(\dfrac{P/A_gE_c}{\varepsilon_o}\right) \leq 1.0$

Notes: For FEMA 356, ASCE 41, and lower-bound methods, p is axial load ratio defined in Eq. (8) and stiffness values are interpolated for axial load ratios falling between limits. For Approximations A and B, ρ is longitudinal reinforcement ratio defined by Eq. (6); n is ratio of steel to concrete elastic moduli; and ε_o is 0.002. Effective shear stiffness of $0.4E_cA_w$ and effective axial stiffness of E_cA_g are used for all analyses, where E_c is elastic modulus of concrete; A_w is shear area; and A_g is gross section area.

demand less than $\phi15A_j\sqrt{f_c'}$, with f_c' in psi ($\phi1.25A_j\sqrt{f_c'}$, with f_c' in MPa), corresponds to $\tau \leq 0.85 \times 15$. The ACI Code requirement of $h_c/d_b > 20$ corresponds to $\lambda \leq 24\sqrt{psi}$ ($1.99\sqrt{MPa}$) for the case of $f_y = 60$ ksi (413 MPa) and $f_c' = 4000$ psi (27.6 MPa). These ACI Code limits are indicated by dashed lines in Fig. 3.

FRAME EFFECTIVE STIFFNESS

A numerical model of a moment-resisting frame typically employs frame-type line elements to represent beams and columns; the physical properties of length, area, moment of inertia, and modulus of elasticity are used to determine the flexural, shear, axial, and torsional stiffness of the element. For RC structures, the elastic modulus of plain concrete is typically used and a reduction factor is applied to the effective stiffness values to account for the flexibility that results from concrete cracking and other softening mechanisms. This reduced stiffness is typically referred to as an effective stiffness and described in terms of a reduction to the cross-sectional properties. For example, an effective axial stiffness might be described as $0.5E_cA_g$, where E_c is the elastic modulus of concrete, and A_g is the gross section area. Recommendations for appropriate effective stiffness values for use in analysis of RC components are provided by codes,[25,27,28] and standards.[13,29]

This study considered effective flexural stiffness recommendations provided by: 1) FEMA 356[24]; 2) ASCE/SEI 41-06[13]; and 3) Elwood and Eberhard.[30,31] Table 2 lists these recommendations. Recommendations for torsional effective stiffness could not be evaluated using the available two-dimensional subassemblage test data and are not listed in Table 2. An effective shear stiffness of $0.4E_cA_w$ and an effective axial stiffness of E_cA_g were used for all analyses, as recommended in both FEMA 356[24] and ASCE/SEI 41-06.[13]

FEMA 356,[24] Section 6.4.1.2.1, specifies, for a linear analysis, the use of the secant stiffness to initial yield as the effective stiffness and provides the recommended values listed in Table 2; these recommendations are referred to as FEMA 356. ASCE/SEI 41-06[13] also specifies the secant stiffness to initial yield as the effective stiffness and provides the values listed in Table 2; these recommendations are referred to as ASCE 41. The ASCE/SEI 41-06[13] commentary on the recommended values cites the work of Elwood and Eberhard,[30] who evaluated the effective stiffness of columns using the PEER Structural Performance Database.[32] The work by Elwood and Eberhard[30] indicates that the lower limit on the ASCE 41 stiffness values could be reduced to $0.2EI_g$; this modification to the ASCE 41 recommendations is listed in Table 2 and is referred to as the lower-bound stiffness. Also evaluated in this study were expressions for approximate flexural stiffness developed by Elwood and Eberhard[31] as a function of axial load and longitudinal reinforcement (referred to as Approximation A) and as a function of axial load with an assumed longitudinal reinforcement ratio (referred to as Approximation B).

RIGID OFFSET MODELS

The beam-column joint region of an RC frame could be expected to exhibit different response mechanisms and be significantly stiffer than the surrounding frame members. Thus, rigid offsets are commonly introduced at the ends of beam and column frame elements within the joint volume. Recommendations for rigid offset lengths are provided in FEMA 356[24] and ASCE/SEI 41-06.[13] Established rigid offset models were evaluated herein using the experimental data set. Revised recommendations for offset lengths were also developed. When combined with the best available effective stiffness models for frame members, these revised recommendations for rigid offset lengths provide improved accuracy in simulating the measured response of frame subassemblages tested under reverse-cyclic lateral loading.

Established rigid offset models

Figure 4 presents the recommendations for rigid offset lengths provided in FEMA 356[24] and ASCE/SEI 41-06.[13] In

FEMA 356,[24] it is recommended that beam and column elements both include rigid offsets that span the entire joint dimension (Fig. 4(a)). ASCE/SEI 41-06[13] recommends that the rigid offset length be determined on the basis of the relative flexural strengths of these elements.[33] For a strong-column, weak-beam design ($\Sigma M_{nc}/\Sigma M_{nb} \geq 1.2$), full rigid offset lengths are used in the columns and no rigid offsets are used in the beams (Fig. 4(b)). For a strong-beam, weak-column design ($\Sigma M_{nc}/\Sigma M_{nb} \leq 0.8$), full rigid offset lengths are used in the beams and rigid offsets are not provided in the columns (Fig. 4(c)). For intermediate cases ($0.8 < \Sigma M_{nc}/\Sigma M_{nb} < 1.2$), both the beams and columns have rigid offset lengths equal to half the joint dimension (Fig. 4(d)).
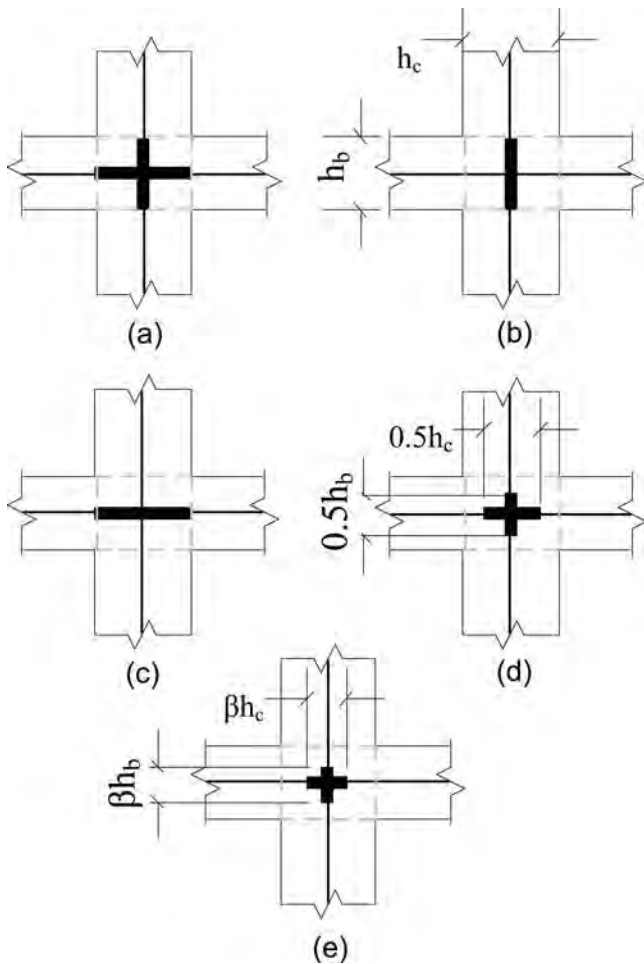

Fig. 4—Offset configuration recommendations of: (a) FEMA 356[24]; (b-d) ASCE/SEI 41-06[13]; and (e) proposed offset length.

Proposed rigid offset length ratio

To improve the accuracy of the linear frame modeling approach, optimal offset length ratios were calibrated using the available experimental data. The beam and column offset lengths were defined as a percentage of the total length, as shown in Fig. 4(e). Two types of expressions were developed. The first expressed the ratio of offset length to joint dimension as a constant value β_{opt}. The second, $\beta_{f()}$, expressed the offset length ratio as a function of design parameters.

Calibration of the proposed offset length expressions was done using the frame-member effective stiffness recommendations discussed previously. This approach assumes that the effective stiffness values for the beams and columns are accurate. As discussed in the following, however, this is not uniformly true; the impact of this on the calibration and evaluation of offset length is also discussed.

Ideal offset lengths

As a preliminary step in developing the offset length recommendations, for each specimen i, the optimal offset length $\beta_{opt}{}^i$ was found. The optimal length was defined as the length required to simulate a column displacement $\Delta_y{}^{sim}$ at the initial yield load V_y, equal to the measured displacement Δ_y. Because rigid offsets essentially define an effective joint size, the optimal offset length for each subassemblage was bounded by a lower limit of 0.0 and an upper limit of 1.0. For any particular specimen, if the effective stiffness used for frame members was too high, the lower-bound offset value was adopted: $\beta_{opt}{}^i = 0$; if the effective stiffness was too low, the upper-bound offset value was adopted: $\beta_{opt}{}^i = 1$.

Table 3 lists a summary of $\beta_{opt}{}^i$ values calculated using the frame-member effective stiffness values in Table 2. Table A3 in the Appendix provides the values for individual specimens. Using ASCE/SEI 41-06[13] stiffness expressions, 21 subassemblages had $\beta_{opt}{}^i = 0$, and 20 had meaningful values for $\beta_{opt}{}^i$ (that is, $0 < \beta_{opt}{}^i < 1$). Using the lower-bound stiffness values, 23 subassemblages had $0 < \beta_{opt}{}^i < 1$. Using the FEMA 356 stiffness recommendations, however, all but one subassemblage had $\beta_{opt}{}^i = 0$ (indicating that the FEMA 356 stiffness are too large); consequently, FEMA 356 values were not considered in developing recommendations for the optimal offset length. The Approximation A and B stiffness values were excluded from further use due to the similarity in the optimal values computed using these and the ASCE 41 stiffness expressions.

Offset ratio expressions

To develop improved recommendations for rigid offset length, a constant-value rigid offset length ratio, β_{opt}, was investigated first. Values were determined using both the ASCE 41 and lower-bound stiffness recommendations. Values of β_{opt} were found for the complete, 45-specimen data

Table 3—Summary of optimal subassemblage rigid offset length ratios

Value	β^i_{opt}				
	FEMA 356	ASCE 41	Lower-bound	$f(\rho_j, p)$	$f(p)$
Minimum	0.02	0.04	0.08	0.03	0.01
Maximum	0.02	0.96	0.98	0.87	0.75
Mean	0.02	0.34	0.66	0.33	0.31
Coefficient of variation	—	0.89	0.45	0.82	0.75
$0 < \beta < 1$	1	23	22	16	20

Notes: Only specimens with $0 < \beta < 1$ are included. Refer to Table A3 in Appendix for values for individual specimens.

set, as well as for subsets of this: 1) ACI-compliant specimens; 2) ACI-noncompliant specimens; 3) brittle specimens as defined by Eq. (10) and (11); and 4) ductile specimens as defined by Eq. (10) and (11). Values were found for the subsets because evaluation of the $\beta_{opt}{}^i$ values listed in Table A3 (in the Appendix) showed that $\beta_{opt}{}^i$ was typically equal to or slightly greater than zero for joints that were either ACI-noncompliant or brittle. To determine the optimal value of β_{opt}, the Matlab Optimization Toolbox (http://matworks.com) was used to minimize the error function

$$\Sigma_{i=1}^{N}(\varepsilon_i)^2 \qquad (12)$$

where

$$\varepsilon_i = \frac{(\Delta_{Yield})^i - (\Delta_{Yield}^{sim})^i}{(\Delta_{Yield})^i} \qquad (13)$$

and $(\Delta_{Yield})^i$ is the measured displacements of specimen i at the initial yield load; $(\Delta_{Yield}{}^{sim})^i$ is the yield displacement simulated using β_{opt}; and N is the number of specimens considered.

The use of a single, constant-value β_{opt} provides the simplest approach for simulating joint stiffness. However, a preliminary review of the computed β_{opt} values and resulting simulated initial yield displacements for the different categories of specimens suggested that, to improve the accuracy of the predicted initial yield displacement, it would be necessary to define the rigid offset length ratio β to be a function of frame design parameters. Thus, a second set of offset length models, $\beta_{f()}$, was developed using linear regression applied to the optimal offset length ratios computed for each specimen, $\beta_{opt}{}^i$, and the joint design parameters in Eq. (1) to (7). In performing the linear regression, only specimens with $0 < \beta_{opt}{}^i < 1$ were used. Because few specimens met this requirement for the lower-bound stiffness recommendations, only the ASCE/SEI 41-06[13] stiffness values were used. Expressions for $\beta_{f()}$ were found for the full data set and the subsets used in calibrating β_{opt}.

Table 4 shows the correlation coefficients R^2 for the linear regression analyses; values greater than 20% were considered to represent a significant correlation between β_{opt} and a specific design parameter. The results indicate that for the full data set, the rigid offset length depends on the bond stress demand λ and beam-bar anchorage length ratio $(h_c/d_b)_{norm}$; the same is also true for the ACI-compliant specimens. For ACI-noncompliant specimens, no significant correlation was observed between $\beta_{opt}{}^i$ and the design parameters considered. For ductile specimens, the offset length ratio $\beta_{opt}{}^i$ was correlated with joint shear stress demand τ, bond stress demand λ, and beam-bar anchorage length ratio $(h_c/d_b)_{norm}$ and joint transverse reinforcement ratio ρ_t. Brittle specimens exhibited the same correlation, with the exception of bond demand. For each subset of the complete data set, the joint design parameters that showed a significant correlation were used to develop the $\beta_{f()}$ offset length expressions. In instances where λ and $(h_c/d_b)_{norm}$ were both significant, only λ was used, as both parameters characterize bond demand. Likewise, only τ was used when both τ and ϕ_j were found to be significant. If two design parameters were determined to be correlated with $\beta_{opt}{}^i$ for a particular data subset, then

Table 4—Correlation coefficient R^2 of rigid offset length ratio versus design parameter from linear regression[*]

	τ	$(h_c/d_b)_{norm}$	λ	ϕ_j	ρ_j	$\Sigma M_{nc}/\Sigma M_{nb}$	p
All	0.10	**0.59**	**0.43**	0.19	0.02	0.14	0.16
ACI-compliant	0.07	**0.92**	**0.79**	**0.05**	0.01	0.13	0.00
ACI-noncompliant	0.09	0.03	0.19	0.12	0.15	0.07	0.00
Ductile	**0.41**	**0.79**	**0.55**	**0.13**	0.01	0.12	0.14
Brittle	**0.83**	**0.90**	0.12	**0.42**	0.14	0.0	0.08

[*]Bold values are considered significant correlation.

$\beta_{f()}$ expressions were developed—first using each parameters individually and then again using both.

It should be noted that in ASCE/SEI 41-06,[13] rigid offset lengths are determined as a function of the relative moment strengths of the beams to the moment strengths of the columns, yet no correlation was found between the ratio of beam-column moments and an offset length that accurately predicted the initial stiffness of the structure.

EVALUATION OF EFFECTIVE FLEXURAL STIFFNESS RECOMMENDATIONS

The experimental data were used first to evaluate the recommendations for the frame-member effective flexural stiffness values listed in Table 2. The measured concrete strength was used to calculate the modulus of elasticity E_c, using the ACI expression,[25] as the design values were not available. The Approximation A and B flexural stiffness values were not evaluated due to similarity with the ASCE 41 values. Two models of each specimen were created: one in which no offsets were used (referred to as the centerline model), and one in which the joint was assumed to be completely rigid and rigid offsets were introduced in both beams and columns with rigid offset lengths equal to the joint dimensions (referred to as the rigid joint model). The stiffness values were evaluated on the basis of the average normalized error in initial yield displacement

$$\overline{\varepsilon} = \frac{1}{N}\Sigma_{i=1}^{N}\varepsilon_i \qquad (14)$$

and the standard deviation in this error

$$\frac{1}{(N-1)^2}\Sigma_{i=1}^{N}(\varepsilon_i - \overline{\varepsilon})^2 \qquad (15)$$

where all parameters are as previously defined in Eq. (12) and (13). A positive average error indicates that, on average, the model is stiffer than the real system, whereas a negative error indicates that it is more flexible. For this study, the preferred effective stiffness model results in a positive average error for the rigid joint model and a negative average error for the centerline model, thus providing an opportunity for improving the accuracy of the simulated initial yield displacement by adjusting the rigid offset length.

Table 5—Initial yield displacement error data for different flexural stiffnesses and centerline and rigid joint models

Data set	Error	FEMA 356		ASCE/SEI 41-06		Lower-bound	
		Centerline	Rigid joint	Centerline	Rigid joint	Centerline	Rigid joint
All	Average	0.38	0.59	0.0	0.35	–0.48	0.04
	Standard deviation	0.15	0.10	0.26	0.17	0.39	0.25
ACI-compliant	Average	0.23	0.50	–0.27	0.17	–0.89	–0.24
	Standard deviation	0.12	0.08	0.20	0.13	0.30	0.19
ACI-noncompliant	Average	0.41	0.61	0.06	0.38	–0.39	0.10
	Standard deviation	0.14	0.09	0.23	0.15	0.35	0.13
Ductile	Average	0.34	0.58	–0.08	0.31	–0.61	–0.02
	Standard deviation	0.15	0.10	0.25	0.17	0.37	0.26
Brittle	Average	0.44	0.62	0.12	0.41	–0.29	0.14
	Standard deviation	0.13	0.09	0.20	0.13	0.29	0.19

Table 5 provides error data for the models considered. The FEMA 356 recommendations result in the stiffest model. Using these recommendations, the average error ranges from 61% using the rigid joint model for specimens with ACI-noncompliant joints to 23% using the centerline model for ACI-compliant specimens. These results were consistent with the observations made by Elwood and Eberhard.[31] Given the large positive average error computed using the FEMA 356 stiffness and the centerline model, no further work was done to calibrate an optimal rigid offset length ratio for use with these frame-member stiffness values.

The data in Table 5 show that the ASCE/SEI 41-06[13] effective stiffnesses represent a significant improvement over the FEMA 356[24] values and suggest frame categories for which improved modeling of joint flexibility can significantly improve the prediction of initial yield displacement. For the full data set and using a fully rigid joint model, the data in Table 5 show that the ASCE 41 stiffness recommendations resulted in an average error of 35% versus 59% when the FEMA 356 recommendations were used. Similarly, for the full data set and the centerline model, ASCE 41 recommendations resulted in an average error of 0% with a standard deviation of 26% versus an average error of 38% with a standard deviation of 15% when the FEMA 356 recommendations were used. For ACI-compliant joints, the ASCE 41 recommendations resulted in a centerline model that was too flexible (average error of –27% with a standard deviation of 23%) and a rigid joint model that was too stiff (average error of 17% with a standard deviation of 13%). These results suggest that for ACI-compliant joints, use of the ASCE 41 stiffness values with a rigid offset length ratio between 0 and 1 can improve the prediction of initial yield displacement. For ACI-noncompliant joints, however, use of the ASCE 41 stiffness values and the centerline model resulted in an average error of 6% with a standard deviation of 23%. Thus, the model provided acceptable accuracy and precision and could not be improved through the introduction of frame-member rigid offsets within the joint volume. Similar results were obtained when specimens were categorized as ductile and brittle. Given the data in Table 5, additional work was done to determine an optimal rigid offset length ratio for use with the ASCE 41 stiffness values for systems with ACI-compliant joints.

Use of the lower-bound flexural stiffness recommendations resulted in models that were significantly more flexible than those resulting from use of the ASCE 41 stiffness recommendations. For the entire data set, the average error in initial yield displacement was –48% for the centerline model and 4% for the rigid joint model. For ACI-compliant joints, use of the lower-bound stiffness values resulted in average errors of –89% for the centerline model and –24% for the rigid joint model; thus, the lower-bound stiffness values were far too low for this category of specimens. For ACI-noncompliant joints, the average errors were –39% for the centerline model and 10% for the rigid joint model; thus, for this category of specimens, the lower-bound stiffness values were reasonable and improved modeling of joint flexibility could improve the prediction of initial yield displacement. Given the data in Table 5, no additional work was done to determine optimal rigid offset lengths for use with the lower-bound stiffness recommendations.

EVALUATION OF RIGID OFFSET MODELS

The experimental data were used to compare the FEMA 356[24] and ASCE/SEI 41-06[13] recommendations for modeling joint stiffness with those developed in this study. As was done in evaluating frame-member effective stiffness recommendations, simulation results were evaluated using Eq. (12) and (13). Table 6 provides the average normalized error in the simulated initial yield displacement and its standard deviation for the models and frame categories considered.

The data in Table 6 show that the FEMA 356 offset recommendations and frame-member stiffness values, used together, resulted in an overly stiff model. The average error for brittle joints was 60%. This result was expected, given the results of the evaluation of the frame-member stiffness values. This further supports the conclusion that the FEMA 356 recommendations are not appropriate for use in simulating concrete frame stiffness.

For the complete data set, the ASCE 41 recommendations for frame-member stiffness and rigid offset lengths within the joint resulted in the overprediction of system stiffness, with an average error of 19%. For specimens with ACI-compliant joints, however, the numerical model was slightly more flexible that the real system, with an average error of –3%. For specimens with ACI-noncompliant joints, however, the model was significantly stiffer than the real system, resulting in an

Table 6—Proposed rigid offset length ratios

Data set	Stiffness	Offsets	Error: average	Error: standard deviation
All	FEMA	FEMA	0.59	0.10
	ASCE	ASCE	0.19	0.21
		$\beta_{opt} = 0.2$	0.08	0.24
		$\beta_{f0} = -0.025\lambda + 0.94$	0.10	0.19
	Lower-bound	$\beta_{opt} = 1.0$	0.04	0.25
ACI-compliant	FEMA	FEMA	0.50	0.08
	ASCE	ASCE	–0.03	0.16
		$\beta_{opt} = 0.6$	0.01	0.16
		$\beta_{f0} = -0.034\lambda + 1.3$	0.04	0.13
	Lower-bound	$\beta_{opt} = 1.0$	–0.24	0.19
ACI-noncompliant	FEMA	FEMA	0.61	0.09
	ASCE	ASCE	0.23	0.19
		$\beta_{opt} = 0.0$	0.06	0.23
	Lower-bound	$\beta_{opt} = 0.9$	0.06	0.23
Ductile	FEMA	FEMA	0.59	0.10
	ASCE	ASCE	0.15	0.20
		$\beta_{opt} = 0.3$	0.07	0.22
		$\beta_{f0} = -0.075\tau + 1.2$	0.07	0.20
		$\beta_{f0} = -0.038\lambda + 1.2$	0.10	0.17
		$\beta_{f0} = -0.068\tau - 0.036\lambda + 1.9$	0.06	0.18
	Lower-bound	$\beta_{opt} = 1.0$	0.0	0.25
Brittle	FEMA	FEMA	0.60	0.11
	ASCE	ASCE	0.24	0.21
		$\beta_{opt} = 0.0$	0.08	0.26
		$\beta_{f0} = 0.11(h_c/d_b)_{norm} - 1.5$	0.13	0.18
	Lower-bound	$\beta_{opt} = 0.8$	0.02	0.27

average error of 23%. When ductile and brittle classifications were considered, the ASCE 41 recommendations resulted in the overprediction of the stiffness of both groups; ductile and brittle joints had average errors of 15% and 24%, respectively.

The data in Table 6 also show that by using the ASCE 41 frame-member stiffness expressions, simulation of system stiffness could be improved. If a constant offset length ratio β_{opt} was used, the error was reduced, for all data sets, to at least half of the error found using the ASCE 41 offset length recommendations. For ACI-compliant joints, an offset length ratio of $\beta_{opt} = 0.6$ resulted in an average error of 1%, with a standard deviation of 16%. For ACI-noncompliant joints, the optimal offset length was found to be zero, producing an average error of 6%. Similarly, for specimens with ductile joints, the use of $\beta_{opt} = 0.3$ resulted in an average error of 7% and for specimens with brittle joints, the use of $\beta_{opt} = 0.0$ resulted in an average error of 8%.

Functional offset length ratios β_{f0} were determined with the goal of further improving modeling. The data in Table 6 show that this was achieved for ductile specimens; definition of the rigid offset length ratio as a function of τ and μ resulted in a reduction in the average normalized initial yield displacement error and its standard deviation. For the complete data set and all other subsets, however, use of the functional ratios resulted in a decrease in the standard deviation of the normalized initial yield displacement error but increased the average error by 2 to 5%.

An additional set of β_{opt} values were calculated using the lower-bound stiffness for frame members. For the full data set, $\beta_{opt} = 1.0$ produced an average error of 4%. For ACI-compliant specimens, $\beta_{opt} = 1.0$ resulted in an overly flexible model and an average error of –25%. For ACI-noncompliant specimens, $\beta_{opt} = 0.9$ produced reasonable results with an average error of 6%. Similarly, for brittle specimens, $\beta_{opt} = 0.8$ resulted in an average error of 2%, whereas for ductile specimens, $\beta_{opt} = 1.0$ resulted in an average error of 0% but a standard deviation of 25%.

RECOMMENDATIONS

The aforementioned research results support two recommendations for linear analysis of RC frames subjected to earthquake loading. The preferred modeling approach uses the ASCE/SEI 41-06[13] frame stiffness values and offset lengths based on compliance with ACI 318-08[25] SMF design requirements

$$\beta_{ASCE\ 41}^{compliant} = 0.6 \qquad (18)$$

$$\beta_{\text{ASCE 41}}^{noncompliant} = 0.0 \qquad (19)$$

This combination provided a good balance of ease of use; accuracy (1% and 6% error for ACI-compliant and ACI-noncompliant specimens, respectively); and precision (standard deviations of 16% for ACI-compliant joints and 23% for ACI-noncompliant joints) while adhering to the standards[13,25] currently used by the industry.

An alternative recommendation can also be considered using the lower-bound frame stiffness recommendations presented by Elwood and Eberhard,[30] with rigid offset lengths dependent on the ductility classification criteria presented in Eq. (10) and (11)

$$\beta_{\text{LowerBound}}^{ductile} = 1.0 \qquad (16)$$

$$\beta_{\text{LowerBound}}^{brittle} = 0.8 \qquad (17)$$

This method for modeling resulted in better accuracy (0% for ductile joints and 2% for brittle joints) than is provided by the preferred approach discussed previously, but was also less precise (25% for ductile joints and 27% for brittle joints) and deviated from the frame stiffness values of ASCE/SEI 41-06[13] and ACI 318-08[25] SMF design guidelines.

SUMMARY AND CONCLUSIONS

Linear models of RC moment frames subjected to cyclic loading were evaluated using a data set of 45 frame subassemblage tests. Recommendations for flexural stiffness of frame members from FEMA 356,[24] ASCE/SEI 41-06,[13] and the work of Elwood and Eberhard[30,31] were evaluated using centerline models and models with a rigid joint. This evaluation showed that the FEMA 356 stiffness values are too large for all systems and that the ASCE 41 and Elwood and Eberhard stiffnesses provided a more accurate simulation of frame-member stiffness. FEMA 356[24] and ASCE/SEI 41-06[13] provide recommendations for frame-member rigid offset lengths to simulate joint flexibility. Evaluation of these recommendations showed that: 1) employing the FEMA 356[24] recommendations of frame-member and joint stiffness resulted in an overly stiff model and highly inaccurate simulation of initial yield displacement; and 2) employing the ASCE/SEI 41-06[13] recommendations for frame-member and joint stiffness resulted in a more flexible model than resulted from application of the FEMA 356[24] recommendations; however, the ASCE/SEI 41-06[13] model was still too stiff for all frame subassemblages, except those with joints meeting the ACI 318-08[25] requirements for SMF. Finally, offset length recommendations were developed to improve the simulation of secant stiffness to initial yield. Offset length recommendations were made on the basis of compliance/noncompliance with ACI 318-08[25] requirements for joints and for joints predicted, on the basis of design shear demand and bond demand, to be ductile or brittle. Evaluation of these new recommendations showed a decrease, in comparison with existing modeling recommendations, in the error in simulated initial yield displacement.

ACKNOWLEDGMENTS

REFERENCES

1. Beckingsale, C. W., "Post-Elastic Behavior of Reinforced Concrete Beam-Column Joints," PhD thesis, Department of Civil Engineering, University of Canterbury, Christchurch, New Zealand, 1980.

2. Otani, S.; Kobayashi, Y.; and Aoyama, H., "Reinforced Concrete Interior Beam-Column Joints under Simulated Earthquake Loading," *U.S.-New Zealand-Japan Seminar on Design of Reinforced Concrete Beam-Column Joints*, Monterey, CA, 1984.

3. Park, R., and Milburn, J. R., "Comparison of Recent New Zealand and United States Seismic Design Provisions for Reinforced Concrete Beam-Column Joints and Test Results from Four Units Designed According to the New Zealand Code," *New Zealand National Society of Earthquake Engineering Bulletin*, V. 16, No. 1, 1983, pp. 3-24.

4. Alire, D., "Seismic Evaluation of Existing Unconfined Reinforced Concrete Beam-Column Joint," MSCE thesis, Department of Civil Engineering, University of Washington, Seattle, WA, 2002, 291 pp.

5. Walker, S., "Seismic Performance of Existing Reinforced Concrete Beam-Column Joints," MSCE thesis, Department of Civil Engineering, University of Washington, Seattle, WA, 2001, 308 pp.

6. Durrani, A. J., and Wight, J. K., "Experimental and Analytical Study of Beam to Column Connections Subjected to Reverse Cyclic Loading," *Technical Report*, Department of Civil Engineering, University of Michigan, Ann Arbor, MI, 1982, 275 pp.

7. Endoh, Y.; Kamura, T.; Otani, S.; and Aoyama, H., "Behavior of RC Beam-Column Connections Using Lightweight Concrete," *Transactions of JCI*, V. 13, 1991, pp. 319-326.

8. Kitayama, K.; Otani, S.; and Aoyama, H., "Earthquake Resistant Design Criteria for Reinforced Concrete Interior Beam-Column Joints," *Pacific Conference on Earthquake Engineering*, Wairakei, New Zealand, 1987, pp. 315-326.

9. Meinheit, D. F., and Jirsa, J. O., "The Shear Strength of Reinforced Concrete Beam-Column Joints," *Technical Report*, University of Texas at Austin, Austin, TX, 1977, 271 pp.

10. Noguchi, N., and Kashiwazaki, T., "Experimental Studies on Shear Performances of RC Interior Column-Beam Joints," *Tenth World Conference on Earthquake Engineering*, Madrid, Spain, 1992, pp. 3163-3168.

11. Park, R., and Ruitong, D., "A Comparison of the Behavior of Reinforced Concrete Beam Column Joints Designed for Ductility and Limited Ductility," *Bulletin of the New Zealand National Society for Earthquake Engineering*, V. 21, No. 4, 1998, pp. 255-278.

12. Oka, H., and Shiohara, H., "Tests on High-Strength Concrete Interior Beam-Column Joint Subassemblages," *Tenth World Conference on Earthquake Engineering*, Madrid, Spain, 1992, pp. 3211-3217.

13. ASCE/SEI Committee 41, "Seismic Rehabilitation of Existing Buildings (ASCE/SEI 41-06)," American Society of Civil Engineers, Reston, VA, 2007, 428 pp.

14. Altoontash, A., and Deierlein, G. D., "A Versatile Model for Beam-Column Joints," *ASCE Structures Congress*, Seattle, WA, 2003.

15. Anderson, M.; Lehman, D.; and Stanton, J., "A Cyclic Shear Stress-Strain Model for Joints without Transverse Reinforcement," *Engineering Structures*, V. 30, No. 4, Apr. 2007, pp. 941-954.

16. Ghobarah, A., and Biddah, A., "Dynamic Analysis of Reinforced Concrete Frames Including Joint Shear Deformation," *Engineering Structures*, V. 21, No. 11, Nov. 1999, pp. 971-987.

17. El-Metwally, S., and Chen, W. F., "Moment-Rotation Modeling of Reinforced Concrete Beam-Column Connections," *ACI Structural Journal*, V. 85, No. 4, July-Aug. 1988, pp. 384-394.

18. Kunnath, S. K., "Macromodel-Based Nonlinear Analysis of Reinforced Concrete Structures," *Structural Engineering Worldwide*, Paper No. T101-5, 1998.

19. Lowes, L. N., and Altoontash, A., "Modeling the Response of Reinforced Concrete Beam-Column Joints," *Journal of Structural Engineering*, ASCE, V. 129, No. 12, 2003, pp. 1686-1697.

20. Lowes, L. N.; Mitra, N.; and Altoontash, A., "A Beam-Column Joint Model for Simulating the Earthquake Response of Reinforced Concrete Frames," Pacific Earthquake Engineering Research Center, Berkeley, CA, 2004, 66 pp.

21. Mitra, N., and Lowes, L. N., "Evaluation, Calibration, and Verification of a Reinforced Concrete Beam-Column Joint," *Journal of Structural Engineering*, ASCE, V. 133, No. 1, 2007, pp. 105-120.

22. Shin, M., and Lafave, J. M., "Modeling of Cyclic Joint Shear Deformation Contributions in RC Beam-Column Connections to Overall Frame Behavior," *Structural Engineering & Mechanics*, V. 18, No. 5, Nov. 2004, pp. 645-669.

23. Birely, A. C.; Lowes, L. N.; and Lehman, D. E., "A Model for Practical Nonlinear Analysis of Reinforced Concrete Frames Including Joint Flexibility," *Engineering Structures*, V. 34, Jan. 2012, pp. 455-465.

24. ASCE, "Pre-Standard and Commentary for the Seismic Rehabilitation of Buildings (FEMA 356)," American Society of Civil Engineers prepared for the Federal Emergency Management Agency, Reston, VA, 2000, 518 pp.

25. ACI Committee 318, "Building Code Requirements for Structural Concrete (ACI 318-08) and Commentary," American Concrete Institute, Farmington Hills, MI, 2008, 473 pp.

26. Joint ACI-ASCE Committee 352, "Recommendations for Design of Beam-Column Connections in Monolithic Reinforced Concrete Structures (ACI 352R-02)," American Concrete Institute, Farmington Hills, MI, 2002, 38 pp.

27. NZS 3101-06, "Concrete Structures Standard," Standards Association of New Zealand, Wellington, New Zealand, 2006.

28. BS EN 1998-6:2005, "Eurocode 8: Design of Structures for Earthquake Resistance," British Standards Institution, London, UK, 2005.

29. ATC 32, "Improved Seismic Design Criteria for California Bridges: Provisional Recommendations," Applied Technology Council, Redwood City, CA, 2000, 365 pp.

30. Elwood, K., and Eberhard, M., "Effective Stiffness of Reinforced Concrete Columns," *PEER Research Digest,* No. 2006-1, Mar. 2006, pp. 1-5.

31. Elwood, K., and Eberhard, M., "Effective Stiffness of Reinforced Concrete Columns," *ACI Structural Journal*, V. 106, No. 4, July-Aug. 2009, pp. 476-484.

32. Berry, M. P.; Parrish, M.; and Eberhard, M. O., *PEER Structural Performance Database User's Manual*, Pacific Earthquake Engineering Research Center, University of California, Berkeley, Berkeley, CA, www.ce.washington.edu/~peera1.

33. Elwood, K. J.; Matamoros, A. B.; Wallace, J. W.; Lehman, D. E.; Heintz, J. A.; Mitchell, A. D.; More, M. A.; Valley, M. T.; Lowes, L. N.; Comartin, C. D.; and Moehle, J. P., "Update of ASCE/SEI 41 Concrete Provisions," *Earthquake Spectra*, V. 23, No. 3, Aug. 2007, pp. 493-523.

NOTES:

Table A1 – Experimental data. (Appendix)

Test Program	Test Specimen	Scale	τ $\sqrt{MPa}$	τ $\sqrt{psi}$	$\left(\dfrac{h_c}{d_b}\right)_{norm}$	λ $\sqrt{psi}$ $(\sqrt{MPa})$	ϕ_j	ρ_j	$\dfrac{\sum M_{nc}}{\sum M_{nb}}$	p
Durrani & Wight (1985)	DWX1	1	1.1	13.3	25.9	23.7 (2.0)	0.4	0.8%	1.6	0.05
	DWX2	1	1.1	13.5	25.9	24.0 (2.0)	0.6	1.6%	1.6	0.06
	DWX3	7/8	0.9	10.5	25.9	25.0 (2.1)	0.5	0.8%	1.3	0.05
Otani, Kobayashi, & Aoyama (1984)	OKAJ1	1/2	1.2	14.7	26.8	13.9 (1.2)	0.2	0.3%	1.5	0.08
	OKAJ2	1/2	1.3	15.2	26.8	23.7 (2.0)	0.4	0.6%	1.5	0.08
	OKAJ3	1/2	1.3	15.2	26.8	23.7 (2.0)	0.9	1.7%	1.5	0.08
	OKAJ4	1/2	1.2	14.7	26.8	13.9 (1.2)	0.2	0.3%	1.8	0.30
	OKAJ5	1/2	1.1	13.8	26.8	21.7 (1.8)	0.2	0.3%	1.2	0.07
Meinheit & Jirsa (1981)	MJ1	7/8	2.2	27	14.4	58.6 (4.9)	0.3	0.5%	0.8	0.40
	MJ2	1 1/4	1.8	21.4	14.4	46.4 (3.9)	0.2	0.5%	1.5	0.25
	MJ3	1 3/8	2.2	26.8	14.4	58.2 (4.8)	0.3	0.5%	1.5	0.39
	MJ5	1 1/4	1.9	23.1	14.4	50.1 (4.2)	0.2	0.5%	1.4	0.04
	MJ6	1 1/4	1.9	13.8	14.4	49.5 (4.1)	0.2	0.5%	1.3	0.48
	MJ12	1 1/4	1.9	23.3	14.4	50.6 (4.2)	0.8	2.4%	1.4	0.30
	MJ13	1 1/4	1.8	21.5	14.4	46.7 (3.9)	0.6	1.5%	1.5	0.25
Alire (2002) & Walker (2001)	PEER14	7/8	0.9	10.5	24.6	28.1 (2.3)	0.0	0.0%	1.0	0.10
	PEER22	1 1/8	1.6	18.7	19.7	31.9 (2.6)	0.0	0.0%	1.0	0.10
	PEER0850	1/2	0.6	7.3	20.6	31.9 (2.6)	0.0	0.0%	0.8	0.10
	PEER0995	3/4	0.9	11.2	20.6	24.3 (2.0)	0.0	0.0%	0.9	0.10
	PEER4150	1 1/8	3.4	40.9	14.9	45.6 (3.8)	0.0	0.0%	0.7	0.10
Park & Ruitong (1988)	PR1	5/8	0.5	5.5	44.2	15.6 (1.3)	1.3	1.3%	1.9	0.02
	PR2	3/4	0.7	8.7	23.7	32.9 (2.7)	1.1	1.6%	1.9	0.03
	PR3	5/8	0.5	6.2	44.2	17.5 (1.5)	0.6	0.6%	1.7	0.02
	PR4	3/4	0.7	8.3	23.7	31.1 (2.6)	0.7	0.8%	1.8	0.03
Noguchi & Kashawazaki (1992)	NKOKJ1	1/2	1.9	13.6	14.6	25.4 (2.1)	0.4	0.8%	1.4	0.12
	NKOKJ3	1/2	1.9	13.9	14.6	20.6 (1.7)	0.3	0.8%	1.5	0.12
	NKOKJ4	1/2	1.9	13.6	14.6	25.4 (2.1)	0.4	0.8%	1.4	0.12
	NKOKJ5	1/2	2.4	28.6	14.6	25.4 (2.1)	0.4	0.8%	1.3	0.12
	NKOKJ6	1/2	2.0	24.3	14.6	29.1 (2.4)	0.4	0.8%	1.3	0.12
Oka & Shiohara (1992)	OSJ1	1/2	1.5	17.5	16.9	20.5 (1.7)	0.5	0.4%	1.8	0.11
	OSJ2	1/2	3.6	43.4	7.2	47.9 (4.0)	0.4	0.4%	0.9	0.11
	OSJ4	1/2	1.6	18.7	20.9	17.5 (1.5)	0.4	0.4%	1.6	0.13
	OSJ5	1/2	2.1	24.7	12.8	28.5 (2.4)	0.4	0.4%	1.4	0.13
	OSJ6	1/2	1.6	18.9	15.9	13.0 (1.1)	0.1	0.2%	1.7	0.12
	OSJ7	1/2	1.2	14	15.9	13.0 (1.1)	0.3	0.4%	2.1	0.12
	OSJ8	3/4	2.0	23.5	19.3	18.1 (1.5)	0.2	0.4%	1.6	0.12
	OSJ10	1/2	2.3	28.3	15.4	32.4 (2.7)	0.3	0.4%	1.3	0.12
	OSJ11	3/4	2.8	34.1	19.2	25.9 (2.2)	0.1	0.4%	1.4	0.12
Kitayama, Otani, & Aoyama (1987)	KOAC1	1/2	0.9	11	25.7	14.4 (1.2)	0.2	0.3%	2.1	0.08
	KOAC3	1/2	0.9	11	30.3	14.4 (1.2)	1.5	2.3%	2.1	0.08
Park & Milburn (1983)	PM1	1	1.3	15.1	42.7	17.6 (1.5)	2.2	3.8%	1.3	0.10
Endoh, et. al (1991)	HC	5/8	1.0	12.3	42.7	12.6 (1.0)	0.1	0.3%	1.6	0.05
	A1	5/8	2.2	27	41.3	40.8 (3.4)	0.1	0.4%	1.4	0.06
Beckingsale (1980)	B11	7/8	0.8	9.1	33.9	14.1 (1.2)	1.9	1.6%	1.4	0.04
	B12	7/8	0.8	9.2	38.3	14.4 (1.2)	1.9	1.6%	1.4	0.04

1

2

3

1

Table A2 – Data classification and experimental yield values. (Appendix)

Test Program	Test Specimen	ACI Compliant	Ductility	Yield Force kips (kN)	Yield Disp in (mm)
Durrani & Wight (1985)	DWX1	No	D	28.8 (128)	0.76 (19.2)
	DWX2	No	D	28.8 (128)	0.76 (19.3)
	DWX3	No	D	22.0 (98)	0.57 (14.5)
Otani, Kobayashi, & Aoyama (1984)	OKAJ1	Yes	D	17.4 (77)	0.50 (12.8)
	OKAJ2	Yes	D	17.4 (77)	0.48 (12.1)
	OKAJ3	Yes	D	17.4 (77)	0.44 (11.1)
	OKAJ4	Yes	D	17.4 (77)	0.40 (10.3)
	OKAJ5	Yes	D	17.5 (78)	0.53 (13.4)
Meinheit & Jirsa (1981)	MJ1	No	B	26.8 (119)	2.23 (56.8)
	MJ2	No	B	34.1 (152)	2.24 (56.9)
	MJ3	No	B	30.0 (133)	2.46 (62.5)
	MJ5	No	B	37.3 (166)	4.20 (106.7)
	MJ6	No	B	40.5 (180)	3.86 (98.1)
	MJ12	No	LD	48.0 (213)	4.51 (114.6)
	MJ13	No	B	38.1 (169)	4.09 (104.0)
Alire (2002) & Walker (2001)	PEER14	No	LD	35.7 (159)	0.48 (12.1)
	PEER22	No	B	73.2 (326)	1.13 (28.6)
	PEER0850	No	D	42.4 (189)	1.19 (30.1)
	PEER0995	No	D	63.2 (281)	0.60 (15.1)
	PEER4150	No	B	126.0 (560)	1.68 (42.7)
Park & Ruitong (1988)	PR1	Yes	D	9.1 (41)	0.23 (5.8)
	PR2	No	D	16.1 (71)	0.61 (15.5)
	PR3	No	D	9.0 (40)	0.25 (6.4)
	PR4	No	D	16.2 (72)	0.56 (14.1)
Noguchi & Kashawazaki (1992)	NKOKJ1	No	B	52.6 (234)	1.12 (28.4)
	NKOKJ3	No	B	67.4 (300)	1.75 (44.3)
	NKOKJ4	No	B	52.5 (234)	1.16 (29.4)
	NKOKJ5	No	B	55.2 (246)	1.67 (42.4)
	NKOKJ6	No	B	48.9 (218)	1.14 (29.1)
Oka & Shiohara (1992)	OSJ1	No	LD	44.7 (199)	0.72 (18.2)
	OSJ2	No	B	61.2 (272)	1.65 (42.0)
	OSJ4	No	LD	49.7 (221)	0.74 (18.9)
	OSJ5	No	B	57.9 (257)	1.04 (26.5)
	OSJ6	No	LD	46.8 (208)	0.73 (18.4)
	OSJ7	Yes	D	36.9 (164)	0.58 (14.7)
	OSJ8	No	LD	57.1 (254)	0.62 (15.7)
	OSJ10	No	B	44.1 (196)	1.05 (26.7)
	OSJ11	No	B	49.3 (219)	0.93 (23.7)
Kitayama, Otani, & Aoyama (1987)	KOAC1	No	D	18.6 (83)	0.51 (12.9)
	KOAC3	Yes	D	18.5 (82)	0.53 (13.4)
Park & Milburn (1983)	PM1	Yes	LD	27.3 (121)	3.73 (94.7)
Endoh, et. al (1991)	HC	No	D	24.2 (108)	0.58 (14.7)
	A1	No	B	31.4 (140)	1.51 (38.4)
Beckingsale (1980)	B11	Yes	D	27.0 (120)	0.56 (14.3)
	B12	Yes	D	37.2 (166)	1.24 (31.5)

2

3

4

1 **Table A3 – Optimal subassemblage rigid offset length ratios (Appendix)**

Test Program	Test Specimen	β_{opt}^i				
		FEMA	ASCE	Lower Bound	$f(\rho_j, p)$	$f(p)$
Durrani & Wight (1985)	DWX1	0	0.08	0.83	0	0
	DWX2	0	0.09	0.84	0	0
	DWX3	0	0.20	0.93	0.05	0.02
Otani, Kobayashi, & Aoyama (1984)	OKAJ1	0	0	0.51	0	0
	OKAJ2	0	0	0.70	0	0
	OKAJ3	0	0.05	0.88	0	0
	OKAJ4	0	0	0.72	0.10	0.45
	OKAJ5	0	0	0.32	0	0
Meinheit & Jirsa (1981)	MJ1	0	0	0.85	1	1
	MJ2	0	0.06	1	0.18	1
	MJ3	0	0	0.88	0	1
	MJ5	0	0	0.30	0	0
	MJ6	0	0	0	0.87	1
	MJ12	0	0	0.14	0	1
	MJ13	0	0	0	0	0.07
Alire (2002) & Walker (2001)	PEER14	0	0	0.77	0.27	0
	PEER22	0	0	0.32	0	0
	PEER0850	0	0	0	0	0
	PEER0995	0	0.05	0.83	0.64	0.08
	PEER4150	0	0	0.74	0	0
Park & Ruitong (1988)	PR1	0	0.86	1	1	0.54
	PR2	0	0.13	1	0	0
	PR3	0	0.89	1	1	0.57
	PR4	0	0.26	1	0.16	0
Noguchi & Kashawazaki (1992)	NKOKJ1	0	0.04	0.96	0	0.09
	NKOKJ3	0	0	0	0	0
	NKOKJ4	0	0	0.88	0	0.01
	NKOKJ5	0	0	0.13	0	0
	NKOKJ6	0	0.15	1	0	0.12
Oka & Shiohara (1992)	OSJ1	0	0.23	1	0.34	0.29
	OSJ2	0	0	0	0	0
	OSJ4	0	0.51	1	0.44	0.60
	OSJ5	0	0.05	0.98	0.16	0.19
	OSJ6	0	0.34	1	0.43	0.40
	OSJ7	0	0.32	1	0.56	0.38
	OSJ8	0.02	1	1	0.14	1
	OSJ10	0	0.14	1	0	0.07
	OSJ11	0	0.71	1	0	0.60
Kitayama, Otani, & Aoyama (1987)	KOAC1	0	0.68	1	0.12	0.42
	KOAC3	0	0.59	1	0.03	0.34
Park & Milburn (1983)	PM1	0	0	0	0	0
Endoh, et. al (1991)	HC	0	0.43	1	0	0.15
	A1	0	0	0.08	0	0
Beckingsale (1980)	B11	0	0.96	1	0.86	0.75
	B12	0	0	0.86	0	0

2

3

4